Journal of Computational and Applied Mathematics 290 (2015) 104–113

Contents lists available at ScienceDirect

Journal of Computational and Applied Mathematics

journal homepage: www.elsevier.com/locate/cam

Construction of B-spline surface with B-spline curves as boundary geodesic quadrilateral

Huogen Yang [a,b,*], Guozhao Wang [a]

[a] Department of Mathematics, Zhejiang University, Hangzhou 310027, China

[b] Faculty of Science, Jiangxi University of Science and Technology, Ganzhou 341000, China

HIGHLIGHTS

- An optimized geometric construction method for B-spline geodesic quadrilateral.
- A practical construction scheme for surface interpolating geodesic quadrilateral.
- The constructed surface and geodesics with low degree.

ARTICLE INFO

Article history:
Received 2 August 2014
Received in revised form 9 May 2015

Keywords:
B-spline surface
Interpolation
Geodesic quadrilateral
Optimization

ABSTRACT

This paper is concerned with construction of a B-spline surface that interpolates a B-spline curvilinear quadrilateral as boundary geodesics. The construction consists of two parts. First, from the corner data (i.e., position, unit tangent vector and curvature at the end points of each curve), a four-quartic B-spline curvilinear quadrilateral with minimum strain energy is constructed to satisfy the constraints of the crossing geodesics on a surface. Second, a tensor-product B-spline surface of degree $(5, 5)$ is constructed to interpolate the quadrilateral as boundary geodesics. The control points of the interpolation surface are determined by two steps, and the surface which adheres to the NURBS standard and employs geometric shape handles meeting the requirements of the design scenario. The method is illustrated with several computational examples.

© 2015 Elsevier B.V. All rights reserved.

1. Introduction

Geodesic on a surface is an intrinsic geometric feature that plays an important role in industrial design [1–3]. In recent years, surface reconstruction from one or several geodesic curves has attracted the attention from many researchers, and both independent and crossing geodesic curves have been considered. In the case of independent curves, several methods have been proposed for the surface interpolating these curves as isoparametric geodesics [4–8]. In the case of crossing curves, Hagen [9] developed a triangular interpolation scheme which results in a triangular surface with geodesic boundary curves. Farouki et al. [10] identified the constraint conditions of the crossing geodesics on a surface, and proposed to construct a quadrilateral and triangular patch interpolating a geodesic quadrilateral [11] and triangle [12] by the Coons method. However, due to the restrictions of the crossing geodesic constraints and the Coons interpolation scheme, the degrees of the geodesic curves and the interpolation patch all are very high. For example with polynomial Bézier geodesic curves,

* Corresponding author at: Faculty of Science, Jiangxi University of Science and Technology, Ganzhou 341000, China. Tel.: +86 0797 8312040; fax: +86 0797 8312040.

E-mail address: yanghuogen@126.com (H. Yang).

http://dx.doi.org/10.1016/j.cam.2015.05.004
0377-0427/© 2015 Elsevier B.V. All rights reserved.

the degree 7 was considered in [11], and the interpolation surface patch is of degree (13, 13). As we know, high degree of the curve/surface may lead inconvenience for curve/surface design, and the probability of success of data exchange will be reduced between different systems, so the curves/surfaces with low degree are more welcomed in the design scenario. Then, the immediate question is whether there are curves and surfaces with lower degree to satisfy the constraints of the crossing geodesic interpolation and meet the requirements of CAD system.

In this paper, we focus on the construction of lower degree surface which has four geodesic boundary curves (boundary geodesic quadrilateral). Particularly, the boundary curves and the interpolation surface all are represented in B-spline form, and the boundary curves are constructed from the *Morphosense* measurements by the method described in [4]. Although the boundary geodesic quadrilateral constructed by the method in [4] does not precisely satisfy the geodesic crossing constraints, it does allow us to determine the corner data (position, unit tangent vector and curvature at the end points of each curve). To achieve the goal of the paper, we split the construction process into two parts. First, from the corner data, we construct a four B-spline curvilinear quadrilateral with minimum strain energy to satisfy the constraints required for the crossing geodesics on a surface. Then a B-spline surface, whose control points are determined by two steps, is constructed to interpolate the quadrilateral as boundary geodesic quadrilateral.

The remainder of this paper is organized as follows. Section 2 introduces some notations, and reviews the constraints for the crossing geodesics on a surface. Section 3 then identifies the constraints for a four-quartic B-spline curvilinear quadrilateral to be the boundary geodesic quadrilateral of a surface, and proposes an optimized geometric construction of a four-quartic B-spline curvilinear quadrilateral. The B-spline surface, which interpolates the quadrilateral as boundary geodesic quadrilateral, is constructed in Section 4. Finally, in Section 5 we summarize the results of this paper.

2. Preliminaries

2.1. Notations

In the following discussion, all curves are free of inflections, all surfaces are considered to be regular and oriented.

The inner and cross product of two vectors $\boldsymbol{u}, \boldsymbol{v}$ is denoted by $\langle \boldsymbol{u}, \boldsymbol{v} \rangle$ and $\boldsymbol{u} \times \boldsymbol{v}$. For a regular and oriented surface $\boldsymbol{R}(u, v)$, the unit normal of each point is defined as $\mathbf{N}(u, v) = \frac{\boldsymbol{R}_u(u,v) \times \boldsymbol{R}_v(u,v)}{\|\boldsymbol{R}_u(u,v) \times \boldsymbol{R}_v(u,v)\|}$. For linearly independent vectors $\boldsymbol{u}, \boldsymbol{v}$ and $\boldsymbol{n}$ such that $\boldsymbol{n} \perp \boldsymbol{u}$ and $\boldsymbol{n} \perp \boldsymbol{v}$, we denote by $(\boldsymbol{u}, \boldsymbol{v})_{\boldsymbol{n}}$ the oriented angle between $\boldsymbol{u}$ and $\boldsymbol{v}$ in the sense of $\boldsymbol{n}$, namely, $\frac{\boldsymbol{n}}{\|\boldsymbol{n}\|} = \frac{\boldsymbol{u} \times \boldsymbol{v}}{\|\boldsymbol{u} \times \boldsymbol{v}\|}$, $\sin(\boldsymbol{u}, \boldsymbol{v})_{\boldsymbol{n}} = \det(\frac{\boldsymbol{u}}{\|\boldsymbol{u}\|}, \frac{\boldsymbol{v}}{\|\boldsymbol{v}\|}, \frac{\boldsymbol{n}}{\|\boldsymbol{n}\|})$ and $\cos(\boldsymbol{u}, \boldsymbol{v})_{\boldsymbol{n}} = \langle \frac{\boldsymbol{u}}{\|\boldsymbol{u}\|}, \frac{\boldsymbol{v}}{\|\boldsymbol{v}\|} \rangle$.

For a space curve $\boldsymbol{r}(t)$, we denote by $\boldsymbol{e}(t)$, $\boldsymbol{n}(t)$ and $\boldsymbol{b}(t)$ the tangent, principal normal and binormal vectors, by $k(t)$ and $\tau(t)$ the curvature and torsion of the curve at the point $\boldsymbol{r}(t)$, respectively. Namely,

$$\begin{aligned} &\boldsymbol{e}(t) = \frac{\boldsymbol{r}'(t)}{\|\boldsymbol{r}'(t)\|}, \qquad \boldsymbol{b}(t) = \frac{\boldsymbol{r}'(t) \times \boldsymbol{r}''(t)}{\|\boldsymbol{r}'(t) \times \boldsymbol{r}''(t)\|}, \qquad \boldsymbol{n}(t) = \boldsymbol{b}(t) \times \boldsymbol{e}(t), \\ &k(t) = \frac{\|\boldsymbol{r}'(t) \times \boldsymbol{r}''(t)\|}{\|\boldsymbol{r}'(t)\|^3}, \qquad \tau(t) = \frac{\det(\boldsymbol{r}'(t), \boldsymbol{r}''(t), \boldsymbol{r}'''(t))}{\|\boldsymbol{r}'(t) \times \boldsymbol{r}''(t)\|^2}. \end{aligned} \tag{1}$$

2.2. Constraints for geodesic boundaries crossing on a surface

Consider, as illustrated in Fig. 1, four regular curves $\boldsymbol{r}_1(u), \boldsymbol{r}_2(v), \boldsymbol{r}_3(u), \boldsymbol{r}_4(v)$ with $u, v \in [0, 1]$, such that $\boldsymbol{r}_1(0) = \boldsymbol{r}_2(0) = P_{00}$, $\boldsymbol{r}_1(1) = \boldsymbol{r}_4(0) = P_{10}$, $\boldsymbol{r}_2(1) = \boldsymbol{r}_3(0) = P_{01}$, $\boldsymbol{r}_3(1) = \boldsymbol{r}_4(1) = P_{11}$. Denote by $\boldsymbol{n}_i(j)$, $k_i(j)$ and $\tau_i(j)$ $(i = 1, \ldots, 4, j = 0, 1)$ the principal normal vectors, curvature and torsion at the two end-points of the curves $\boldsymbol{r}_i$, by $A_{00} = (\boldsymbol{r}_1'(0), \boldsymbol{r}_2'(0))_{\mathbf{N}(P_{00})}$, $A_{01} = (\boldsymbol{r}_3'(0), \boldsymbol{r}_2'(1))_{\mathbf{N}(P_{01})}$, $A_{10} = (\boldsymbol{r}_1'(1), \boldsymbol{r}_4'(0))_{\mathbf{N}(P_{10})}$, $A_{11} = (\boldsymbol{r}_3'(1), \boldsymbol{r}_4'(1))_{\mathbf{N}(P_{11})}$ the oriented angles between the two tangent vectors at the corner P_{lj} $(l, j = 0, 1)$, where $\mathbf{N}(P_{lj})$ is the unit normal vector which defines the orientation of the interpolation surface at each corner, i.e.,

$$\begin{aligned} &\mathbf{N}(P_{00}) = \frac{\boldsymbol{r}_1'(0) \times \boldsymbol{r}_2'(0)}{\|\boldsymbol{r}_1'(0) \times \boldsymbol{r}_2'(0)\|}, \qquad \mathbf{N}(P_{01}) = \frac{\boldsymbol{r}_3'(0) \times \boldsymbol{r}_2'(1)}{\|\boldsymbol{r}_3'(0) \times \boldsymbol{r}_2'(1)\|}, \\ &\mathbf{N}(P_{10}) = \frac{\boldsymbol{r}_1'(1) \times \boldsymbol{r}_4'(0)}{\|\boldsymbol{r}_1'(1) \times \boldsymbol{r}_4'(0)\|}, \qquad \mathbf{N}(P_{11}) = \frac{\boldsymbol{r}_3'(1) \times \boldsymbol{r}_4'(1)}{\|\boldsymbol{r}_3'(1) \times \boldsymbol{r}_4'(1)\|}. \end{aligned} \tag{2}$$

For the above four curves, Farouki et al. identified the conditions for them to constitute geodesic boundaries of a surface as follows.

Proposition 1 (*See [10]*)**.** *There exists a regular oriented surface $\boldsymbol{R}(u, v)$ interpolating the four curves as geodesic boundaries if and only if these curves satisfy the following constraints* (C1)–(C3)*:*

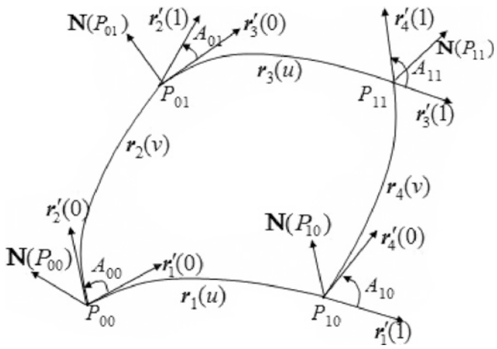

Fig. 1. Patch boundaries and the vectors at the corners.

(C1) *The osculating constraints: The principal normals of the boundary curves that meet at each corner must agree modulo sign. That is, there must exist $\sigma_i(j) \in \{-1, +1\}$, $i = 1, \ldots, 4, j = 0, 1$, such that*

$$\begin{aligned} &\mathbf{N}(P_{00}) = \sigma_1(0)\boldsymbol{n}_1(0) = \sigma_2(0)\boldsymbol{n}_2(0), \qquad \mathbf{N}(P_{01}) = \sigma_2(1)\boldsymbol{n}_2(1) = \sigma_3(0)\boldsymbol{n}_3(0), \\ &\mathbf{N}(P_{10}) = \sigma_1(1)\boldsymbol{n}_1(1) = \sigma_4(0)\boldsymbol{n}_4(0), \qquad \mathbf{N}(P_{11}) = \sigma_3(1)\boldsymbol{n}_3(1) = \sigma_4(1)\boldsymbol{n}_4(1). \end{aligned} \tag{3}$$

(C2) *The global normal orientation constraint: Along the boundary curves, a continuous unit normal vector* $\mathbf{N}$ *of the interpolation surface must exist, such that* $\mathbf{N} = \pm\boldsymbol{n}$ *(*$\boldsymbol{n}$ *is the principal normal vector along the boundary curves).*

(C3) *Geodesic crossing constraints: At each corner, the curvature and torsion must satisfy*

$$\begin{aligned} &P_{00} : [\sigma_1(0)k_1(0) - \sigma_2(0)k_2(0)] \cos A_{00} + [\tau_1(0) + \tau_2(0)] \sin A_{00} = 0, \\ &P_{01} : [\sigma_3(0)k_3(0) - \sigma_2(1)k_2(1)] \cos A_{01} + [\tau_3(0) + \tau_2(1)] \sin A_{01} = 0, \\ &P_{11} : [\sigma_3(1)k_3(1) - \sigma_4(1)k_4(1)] \cos A_{11} + [\tau_3(1) + \tau_4(1)] \sin A_{11} = 0, \\ &P_{10} : [\sigma_1(1)k_1(1) - \sigma_4(0)k_4(0)] \cos A_{10} + [\tau_1(1) + \tau_4(0)] \sin A_{10} = 0. \end{aligned} \tag{4}$$

3. Quartic B-spline curvilinear geodesic quadrilateral

Based on the corner data, in this section, we consider the constraints and construction for a quadrilateral, composed of four B-Spline curves with minimum strain energy, as boundary geodesics of a patch. Since the interpolation condition has the expression of cross product $\boldsymbol{r}' \times \boldsymbol{r}''$ of the geodesic curve $\boldsymbol{r}$ (see Section 4.1), in order to ensure the interpolation surface of low degree and some continuity order, we choose quartic B-spline curves with C^3 continuity. They are defined as follows:

$$\boldsymbol{r}_i(u) = \sum_{j=0}^{7} P_j^i N_{j,4}(u) \quad (i = 1, 3) \quad \text{and} \quad \boldsymbol{r}_i(v) = \sum_{j=0}^{7} P_j^i N_{j,4}(v) \quad (i = 2, 4) \tag{5}$$

where P_j^i are the control points, $P_0^1 = P_0^2 = P_{00}, P_7^2 = P_0^3 = P_{01}, P_7^3 = P_7^4 = P_{11}, P_7^1 = P_0^4 = P_{10}$. $N_{j,4}(u)$ and $N_{j,4}(v)$ are the B-spline bases over the knot vector $\boldsymbol{U} = \{u_0, u_1, \ldots, u_{12}\}$ and $\boldsymbol{V} = \{v_0, v_1, \ldots, v_{12}\}$, respectively, and $u_0 = \cdots = u_4 = 0 = v_0 = \cdots = v_4, u_8 = \cdots = u_{12} = 1 = v_8 = \cdots = v_{12}, u_k < u_{k+1}$ $(k = 4, \ldots, 7)$, $v_l < v_{l+1}$ $(l = 4, \ldots, 7)$. Unless specially declared, the left and right end-knots of the knot vector, mentioned in the rest of this paper, are zero and one, respectively, and their multiplicities are one greater than the degree of the B-spline curve. The strain energy of the four curves is defined as follows (see [13]):

$$\int_0^1 (\|\boldsymbol{r}_1''(u)\|^2 + \|\boldsymbol{r}_3''(u)\|^2)du + \int_0^1 (\|\boldsymbol{r}_2''(v)\|^2 + \|\boldsymbol{r}_4''(v)\|^2)dv. \tag{6}$$

3.1. Constraints for quartic B-spline curvilinear geodesic quadrilateral

(1) *Osculating constraints*

For example, at the corner P_{00}, the osculating constraints are satisfied, that is, the principal normal vectors $\boldsymbol{n}_1(0)$ and $\boldsymbol{n}_2(0)$ are parallel to the orientation unit normal $\mathbf{N}(P_{00}) = \frac{\boldsymbol{r}_1'(0)\times\boldsymbol{r}_2'(0)}{\|\boldsymbol{r}_1'(0)\times\boldsymbol{r}_2'(0)\|}$ of the interpolation surface at the corner P_{00} (see Fig. 2). Then the osculating plane Π_{01} of $\boldsymbol{r}_1(u)$ at the point P_{00} can be determined by $\boldsymbol{r}_1'(0)$ (parallel to $\overrightarrow{P_0^1P_1^1}$) and $\boldsymbol{r}_1'(0) \times \boldsymbol{r}_2'(0)$ (parallel to $\overrightarrow{P_0^1P_1^1} \times \overrightarrow{P_0^2P_1^2}$). Note that $\boldsymbol{r}_1'(0) \times \boldsymbol{r}_1''(0)$, namely, $\overrightarrow{P_0^1P_1^1} \times \overrightarrow{P_1^1P_2^1}$ is orthogonal to Π_{01}, so the control point P_2^1 must be

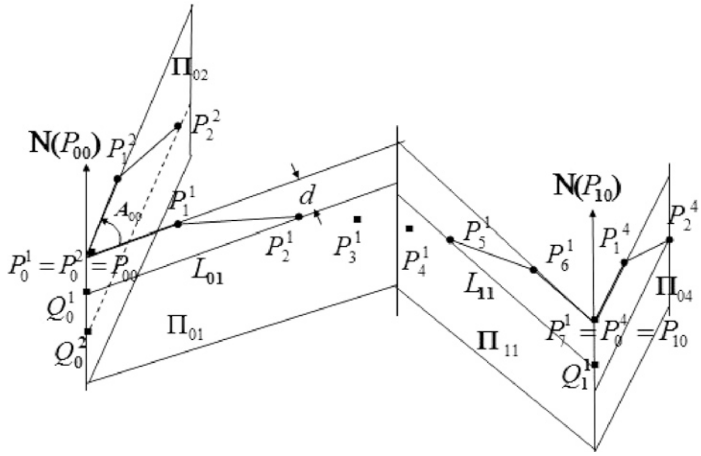

Fig. 2. The location of the control point $P_2^1(\sigma_1(0)=\sigma_2(0)=-1)$.

located in the osculating plane Π_{01}. Similarly, the control point P_2^2 is located in the osculating plane Π_{02} determined by $\boldsymbol{r}_2'(0)$ and $\boldsymbol{r}_1'(0)\times\boldsymbol{r}_2'(0)$ at the corner P_{00}. Then for all corners, osculating constraints are satisfied if and only if the control points P_2^i and P_5^i are located in the osculating plane Π_{0i} and Π_{1i} of the curve $\boldsymbol{r}_i$ at the two end-points, respectively. The osculating plane is determined by the tangent vector of the curve $\boldsymbol{r}_i$ and the orientation unit normal vector at the end-point.

Denote by d_{0i} and d_{1i} the distance of the control point P_2^i to the line $P_0^iP_1^i$ and the control point P_5^i to the line $P_6^iP_7^i$. Because the corner data are fixed, according to [14], d_{0i} and d_{1i} are fixed. That is, the control points P_2^i and P_5^i are always located on two fixed lines L_{0i} and L_{1i}, respectively. Line L_{0i} is parallel to line $P_0^iP_1^i$, the distance between them is d_{0i}, line L_{1i} is parallel to line $P_6^iP_7^i$, and the distance between them is d_{1i}. Let $t_j^i=u_j$ for $i=1,3$, $t_j^i=\upsilon_j$ for $i=2,4,\ j=0,1,\ldots,12$, we have

$$d_{0i}=\frac{4t_6^ik_i(0)}{3t_5^i}\|\overrightarrow{P_0^iP_1^i}\|^2,\qquad d_{1i}=\frac{4(1-t_6^i)k_i(1)}{3(1-t_7^i)}\|\overrightarrow{P_6^iP_7^i}\|^2. \tag{7}$$

Let $Q_0^i=P_0^i+\sigma_i(0)d_{0i}\mathbf{N}(P_0^i)$, $Q_1^i=P_7^i+\sigma_i(1)d_{1i}\mathbf{N}(P_7^i)$, then the points Q_0^i and Q_1^i are located in the osculating plane Π_{0i} and Π_{1i}, the point Q_0^i and P_2^i are located at the same side of the line $P_0^iP_1^i$, and the distances of them to the line $P_0^iP_1^i$ all are d_{0i}. The point Q_1^i has similar conclusion. So the lines L_{0i} and L_{1i} can be expressed as

$$\begin{aligned}L_{0i}:\ &\frac{x-x_{Q_0^i}}{X_{0i}}=\frac{y-y_{Q_0^i}}{Y_{0i}}=\frac{z-z_{Q_0^i}}{Z_{0i}},\\ L_{1i}:\ &\frac{x-x_{Q_1^i}}{X_{1i}}=\frac{y-y_{Q_1^i}}{Y_{1i}}=\frac{z-z_{Q_1^i}}{Z_{1i}},\end{aligned} \tag{8}$$

where

$$\overrightarrow{P_0^iP_1^i}=(X_{0i},Y_{0i},Z_{0i}),\qquad \overrightarrow{P_6^iP_7^i}=(X_{1i},Y_{1i},Z_{1i}),$$
$$Q_0^i=(x_{Q_0^i},y_{Q_0^i},z_{Q_0^i}),\qquad Q_1^i=(x_{Q_1^i},y_{Q_1^i},z_{Q_1^i}).$$

(2) *Global normal orientation constraint*

Due to the interpolating surface orientation and the curve $\boldsymbol{r}_i$ free of inflections, both the unit normal $\mathbf{N}$ of the surface and the principal normal $\boldsymbol{n}$ of each curve are globally continuous. Then the global normal orientation constraint shows such a fact: For $\mathbf{N}=\boldsymbol{n}$ or $\mathbf{N}=-\boldsymbol{n}$, only one of the two holds along each boundary curve. Therefore, the sudden reversal of the principal normal can only occur at four corners, and the number of reversals is even. Namely,

$$\prod_{i,j}\sigma_i(j)=1,\quad i=1,\ldots,4,\ j=0,1. \tag{9}$$

(3) *Corner geodesic crossing constraints*

Let

$$S_0^i=\overrightarrow{P_0^iP_1^i}\times\overrightarrow{P_0^iQ_0^i},\qquad S_1^i=\overrightarrow{P_6^iP_7^i}\times\overrightarrow{P_7^iQ_7^i},$$
$$h_0^i=\frac{(t_5^i)^3}{(t_6^i)^2t_7^ik_i^2(0)}\|\overrightarrow{P_0^iP_1^i}\|^6,\qquad h_1^i=\frac{(1-t_7^i)^3}{(1-t_6^i)^2(1-t_5^i)k_i^2(1)}\|\overrightarrow{P_6^iP_7^i}\|^6,$$
$$g_{mn}^i=\frac{32cotAmn}{9}(\sigma_{i+1}(m)k_{i+1}(m)-\sigma_i(n)k_i(n)),\qquad \sigma_5(1)=\sigma_1(1),\qquad k_5(1)=k_1(1).$$

We then have

Theorem 1. *Corner geodesic crossing constraints (4) are equivalent to*

$$\begin{cases} h_0^1\langle S_0^1, \overrightarrow{P_0^1P_3^1}\rangle + h_0^2\langle S_0^2, \overrightarrow{P_0^2P_3^2}\rangle = g_{00}^1, \\ h_0^3\langle S_0^3, \overrightarrow{P_0^3P_3^3}\rangle + h_1^2\langle S_1^2, \overrightarrow{P_4^2P_7^2}\rangle = -g_{01}^2, \\ h_1^3\langle S_1^3, \overrightarrow{P_4^3P_7^3}\rangle + h_1^4\langle S_1^4, \overrightarrow{P_4^4P_7^4}\rangle = g_{11}^3, \\ h_1^1\langle S_1^1, \overrightarrow{P_4^1P_7^1}\rangle + h_0^4\langle S_0^4, \overrightarrow{P_0^4P_3^4}\rangle = -g_{10}^4. \end{cases} \tag{10}$$

Proof. Because

$$\overrightarrow{P_0^iP_1^i} \times \overrightarrow{P_0^iP_2^i} = \overrightarrow{P_0^iP_1^i} \times \overrightarrow{P_0^iQ_0^i}, \qquad \|\overrightarrow{P_0^iP_1^i} \times \overrightarrow{P_0^iP_2^i}\|^2 = \frac{16(t_6^i)^2}{9(t_5^i)^2}k_i^2(0)\|\overrightarrow{P_0^iP_1^i}\|^6,$$

$$\overrightarrow{P_6^iP_7^i} \times \overrightarrow{P_5^iP_7^i} = \overrightarrow{P_7^iQ_1^i} \times \overrightarrow{P_6^iP_7^i}, \qquad \|\overrightarrow{P_6^iP_7^i} \times \overrightarrow{P_5^iP_7^i}\|^2 = \frac{16(1-t_6^i)^2}{9(1-t_7^i)^2}k_i^2(1)\|\overrightarrow{P_6^iP_7^i}\|^6.$$

Substituting these expressions into the torsion expression in (1) and constraint (4), by direct calculation, Eq. (10) is obtained. □

When the global normal orientation constraint is satisfied and the corner data are fixed, the torsion, that is, the control points P_3^i and P_4^i are not free, they should satisfy Eq. (10). Considering the four curves with minimum strain energy, the control points P_2^i, P_3^i, P_4^i and P_5^i can be obtained by minimizing (6) with the linear constraints (8) and (10).

3.2. Construction of quartic B-spline curvilinear geodesic quadrilateral

According to the above analysis, we now propose an optimized geometric construction for a quadrilateral, composed of four Quartic B-Spline curves with the constraints of the surface geodesic quadrilateral. The construction consists of the following six steps.

(1) *The magnitude of the tangent vectors at both ends are freely chosen, then from the corner data, the control points* P_0^i, P_1^i *and* P_6^i, P_7^i *can be determined.*
(2) *According to* Eqs. (2), *the orientation unit normal vector* $\mathbf{N}(P_{lj})$ *of the interpolation surface is assigned at each corner, defining the orientation of the surface.*
(3) *A sequence of signs* $\sigma_i(0)$ *and* $\sigma_i(1)$ *is chosen, compatible with the global normal orientation constraint* (9).
(4) *According to* Eqs. (8), *the straight line* L_{0i} *and* L_{1i} *are determined.*
(5) *Determining* Eq. (10).
(6) *Minimizing* (6) *with the linear constraints* (8) *and* (10), *the control points* P_2^i, P_3^i, P_4^i *and* P_5^i *are determined.*

Fig. 3 shows three examples of the quartic B-spline quadrilateral with control polygon, constructed in the above manner.

4. B-spline surface interpolating the geodesic quadrilateral

Let t be either of the parametric variables u or v, $\boldsymbol{T}_i = \{t_0^i, t_1^i, \ldots, t_{12}^i\}$, $i = 1, 2, 3, 4$. We now construct a B-spline surface that interpolates the above constructed quadrilateral as geodesic boundaries.

4.1. Compatibility of interpolation conditions

Along the boundary geodesic $\boldsymbol{r}_i(t)$, the transverse tangent vector $\boldsymbol{D}_i(t)$ of the interpolation patch is coplanar with the vector $\boldsymbol{r}_i'(t)$ and $\boldsymbol{r}_i'(t) \times \boldsymbol{r}_i''(t)$, so there exist scalar functions $x_i(t)$ and $y_i(t)$ such that

$$\boldsymbol{D}_i(t) = x_i(t)\boldsymbol{r}_i'(t) + y_i(t)\boldsymbol{r}_i'(t) \times \boldsymbol{r}_i''(t), \quad t \in [0, 1]. \tag{11}$$

Due to a cancellation of leading coefficients, the actual degree of the cross product $\boldsymbol{r}_i'(t) \times \boldsymbol{r}_i''(t)$ is of 4. Taking the compatibility of the interpolation condition (11) at the corner and the degree and continuity of $\boldsymbol{D}_i(t)$ into consideration, we choose $x_i(t) = \sum_{j=0}^{5} a_j^i N_{j,2}(t)$ and $y_i(t) = b_0^i(1-t) + b_1^i t = \sum_{j=0}^{1} b_j^i N_{j,1}(t)$, B-spline basis functions $N_{j,1}(t)$ defined on the knot vector $\boldsymbol{T}_0 = \{0, 0, 1, 1\}$, and B-spline basis functions $N_{j,2}(t)$ of $x_i(t)$ defined on the knot vector $\boldsymbol{T}_i' = \{0, 0, 0, t_5^i, t_6^i, t_7^i, 1, 1, 1\}$.

The interpolation condition (11) must satisfy the compatibility constraints of the corner, which limit the options of the coefficients a_j^i and b_j^i. Consider, for example, the curve $\boldsymbol{r}_1(t)$ at the corner P_0^1 and P_7^1.

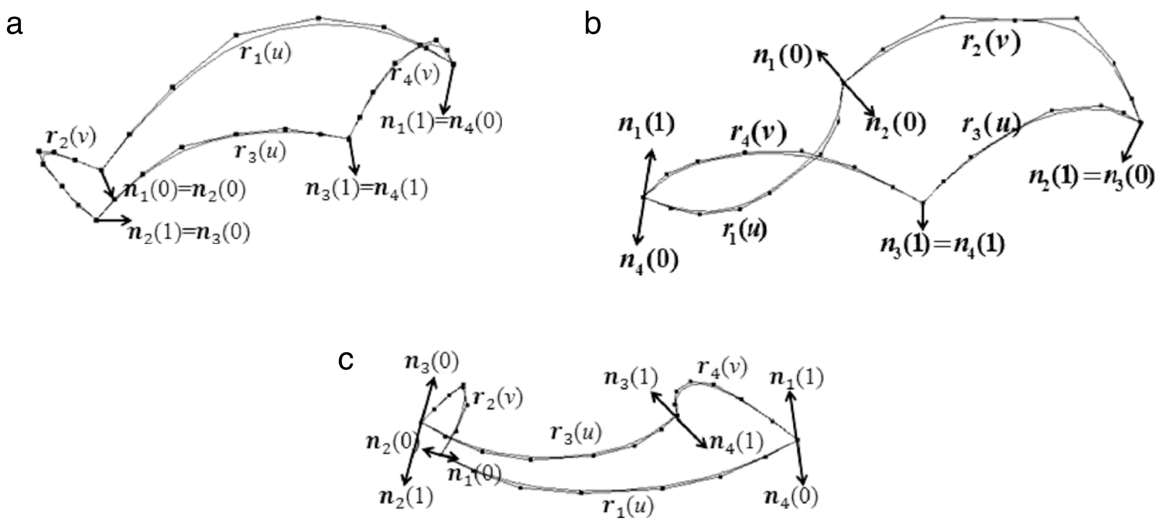

Fig. 3. Four-quartic B-spline curvilinear quadrilateral with control polygon. (a) Principal normal vector with no reversal. (b) Principal normal vector with two reversals. (c) Principal normal vector with four reversals.

(1) Compatibility of tangent vectors

As the transverse tangent vector $\boldsymbol{D}_1(t)$ must interpolate the tangent vector of the curve $\boldsymbol{r}_2(t)$ and $\boldsymbol{r}_4(t)$ at the corner P_0^1 and P_7^1, respectively. Let $i = 1$, $t = 0$ in (11), we have

$$\frac{a_0^1}{u_5}\overrightarrow{P_0^1P_1^1} + \frac{12b_0^1}{u_5^2u_6}\overrightarrow{P_0^1P_1^1} \times \overrightarrow{P_1^1P_2^1} = \frac{1}{v_5}\overrightarrow{P_0^2P_1^2}. \tag{12}$$

Because $\boldsymbol{r}_1'(0)$, $\boldsymbol{r}_2'(0)$ and $\boldsymbol{r}_1'(0) \times \boldsymbol{r}_1''(0)$ are coplanar, Eq. (12) admits solutions as

$$\begin{aligned} a_0^1 &= \frac{u_5}{v_5}\frac{\langle\overrightarrow{P_0^1P_1^1}, \overrightarrow{P_0^2P_1^2}\rangle}{\|\overrightarrow{P_0^1P_1^1}\|^2}, \\ b_0^1 &= \frac{u_5^2u_6}{12v_5}\frac{\det(\overrightarrow{P_0^1P_1^1}, \overrightarrow{P_1^1P_2^1}, \overrightarrow{P_0^2P_1^2})}{\|\overrightarrow{P_0^1P_1^1} \times \overrightarrow{P_1^1P_2^1}\|^2}. \end{aligned} \tag{13}$$

Let $t = 1$ in (11), in the same way, a_5^1 and b_1^1 are determined by

$$\begin{aligned} a_5^1 &= \frac{1-u_7}{v_5}\frac{\langle\overrightarrow{P_6^1P_7^1}, \overrightarrow{P_0^4P_1^4}\rangle}{\|\overrightarrow{P_6^1P_7^1}\|^2}, \\ b_1^1 &= \frac{-(1-u_7)^2(1-u_6)}{12v_5}\frac{\det(\overrightarrow{P_6^1P_7^1}, \overrightarrow{P_5^1P_6^1}, \overrightarrow{P_0^4P_1^4})}{\|\overrightarrow{P_6^1P_7^1} \times \overrightarrow{P_5^1P_6^1}\|^2}. \end{aligned} \tag{14}$$

Similarly solutions for $i = 2, 3, 4$ can be obtained, thus the coefficients a_0^i and a_5^i of $x_i(t)$ and all the coefficients of $y_i(t)$ are determined.

(2) Compatibility of twist vectors

Denote by $\boldsymbol{R}(u, v)$ the interpolation surface. At the corner P_0^1, differentiate $\boldsymbol{D}_1(u)$ and $\boldsymbol{D}_2(v)$, and set $u = 0$ and $v = 0$, we must have

$$\boldsymbol{D}_1'(0) = \boldsymbol{R}_{u,v}(0, 0) = \boldsymbol{D}_2'(0). \tag{15}$$

To compare $\boldsymbol{D}_1'(0)$ and $\boldsymbol{D}_2'(0)$, we consider their projections on the three linearly-independent vectors $\boldsymbol{r}_1'(0)$, $\boldsymbol{r}_2'(0)$ and unit normal $\mathbf{N}(P_0^1)$. Notice that

$$\begin{aligned} \mathbf{N}(P_0^1) &= \sigma_1(0)\frac{(\boldsymbol{r}_1'(0) \times \boldsymbol{r}_1''(0)) \times \boldsymbol{r}_1'(0)}{\|(\boldsymbol{r}_1'(0) \times \boldsymbol{r}_1''(0)) \times \boldsymbol{r}_1'(0)\|} = \sigma_2(0)\frac{(\boldsymbol{r}_2'(0) \times \boldsymbol{r}_2''(0)) \times \boldsymbol{r}_2'(0)}{\|(\boldsymbol{r}_2'(0) \times \boldsymbol{r}_2''(0)) \times \boldsymbol{r}_2'(0)\|}, \\ \sigma_1(0) &= \frac{\|\boldsymbol{r}_1'(0) \times \boldsymbol{r}_2'(0)\|\,\|\boldsymbol{r}_1'(0) \times \boldsymbol{r}_1''(0)\|}{\|\boldsymbol{r}_1'(0)\|\det(\boldsymbol{r}_1'(0), \boldsymbol{r}_2'(0), \boldsymbol{r}_1''(0))}, \qquad \sigma_2(0) = \frac{\|\boldsymbol{r}_1'(0) \times \boldsymbol{r}_2'(0)\|\,\|\boldsymbol{r}_2'(0) \times \boldsymbol{r}_2''(0)\|}{\|\boldsymbol{r}_2'(0)\|\det(\boldsymbol{r}_2'(0), \boldsymbol{r}_2''(0), \boldsymbol{r}_1'(0))}. \end{aligned}$$

Utilizing the curvature and torsion expressions in (1), (13) together with the identity $(\boldsymbol{u}\times\boldsymbol{v})\times\boldsymbol{w}=\langle\boldsymbol{u},\boldsymbol{w}\rangle\boldsymbol{v}-\langle\boldsymbol{v},\boldsymbol{w}\rangle\boldsymbol{u}$, by calculation, we have

• Projection on $\mathbf{N}(P_0^1)$

$$\langle\boldsymbol{D}_1'(0),\mathbf{N}(P_0^1)\rangle=\|\boldsymbol{r}_1'(0)\|\,\|\boldsymbol{r}_2'(0)\|\,[\sigma_1(0)k_1(0)\cos A_{00}+\tau_1(0)\sin A_{00}],$$
$$\langle\boldsymbol{D}_2'(0),\mathbf{N}(P_0^1)\rangle=\|\boldsymbol{r}_1'(0)\|\,\|\boldsymbol{r}_2'(0)\|\,[\sigma_2(0)k_2(0)\cos A_{00}-\tau_2(0)\sin A_{00}].$$

As the corner geodesic crossing constraint is satisfied, $\langle\boldsymbol{D}_1'(0),\mathbf{N}(P_0^1)\rangle=\langle\boldsymbol{D}_2'(0),\mathbf{N}(P_0^1)\rangle$ holds naturally.

• Projection on $\boldsymbol{r}_1'(0)$

$$\begin{aligned}\langle\boldsymbol{D}_1'(0),\boldsymbol{r}_1'(0)\rangle &= \frac{2(a_1^1-a_0^1)}{u_5}\|\boldsymbol{r}_1'(0)\|^2+a_0^1\langle\boldsymbol{r}_1'(0),\boldsymbol{r}_1''(0)\rangle\\ &= \frac{16}{u_5}\left(\frac{2a_1^1}{u_5^2}\|\overrightarrow{P_0^1P_1^1}\|^2+c\right).\end{aligned}$$
$$\langle\boldsymbol{D}_2'(0),\boldsymbol{r}_1'(0)\rangle=\frac{16}{u_5}\left(\frac{2}{v_5^2}\langle\overrightarrow{P_0^1P_1^1},\overrightarrow{P_0^2P_1^2}\rangle a_1^2+d\right),$$

where

$$c=\frac{3a_0^1}{u_5u_6}\langle\overrightarrow{P_0^1P_1^1},\overrightarrow{P_1^1P_2^1}\rangle-\frac{5a_0^1}{u_5^2}\|\overrightarrow{P_0^1P_1^1}\|^2,$$
$$\begin{aligned}d\;=\;&\frac{3a_0^2}{v_5v_6}\langle\overrightarrow{P_0^1P_1^1},\overrightarrow{P_1^2P_2^2}\rangle+\left[\frac{12(b_1^2-b_0^2)}{v_5^2v_6}-\frac{24b_0^2}{v_5^2v_6}\left(\frac{1}{v_5}+\frac{1}{v_6}\right)\right]\det(\overrightarrow{P_0^2P_1^2},\overrightarrow{P_1^2P_2^2},\overrightarrow{P_0^1P_1^1})\\&-\frac{5a_0^2}{v_5^2}\langle\overrightarrow{P_0^1P_1^1},\overrightarrow{P_0^2P_1^2}\rangle+\frac{24b_0^2}{v_5^2v_6v_7}\det(\overrightarrow{P_0^2P_1^2},\overrightarrow{P_2^2P_3^2},\overrightarrow{P_0^1P_1^1}).\end{aligned}$$

• Projection on $\boldsymbol{r}_2'(0)$

$$\langle\boldsymbol{D}_1'(0),\boldsymbol{r}_2'(0)\rangle=\frac{16}{v_5}\left(\frac{2}{u_5^2}\langle\overrightarrow{P_0^1P_1^1},\overrightarrow{P_0^2P_1^2}\rangle a_1^1+e\right),$$
$$\langle\boldsymbol{D}_2'(0),\boldsymbol{r}_2'(0)\rangle=\frac{16}{v_5}\left(\frac{2}{v_5^2}\|\overrightarrow{P_0^2P_1^2}\|^2a_1^2+f\right),$$

where e can be obtained with v and superscript 1, 2 of d replaced by u and superscript 2, 1, f can be obtained with u and superscript 1 of c replaced by v and superscript 2.

Thus, $\boldsymbol{D}_1'(0)=\boldsymbol{D}_2'(0)$ holds if and only if the following linear system of equation admits solutions.

$$\begin{pmatrix}\frac{2}{u_5^2}\|\overrightarrow{P_0^1P_1^1}\|^2 & -\frac{2}{v_5^2}\langle\overrightarrow{P_0^1P_1^1},\overrightarrow{P_0^2P_1^2}\rangle\\ \frac{2}{u_5^2}\langle\overrightarrow{P_0^1P_1^1},\overrightarrow{P_0^2P_1^2}\rangle & -\frac{2}{v_5^2}\|\overrightarrow{P_0^2P_1^2}\|^2\end{pmatrix}\begin{pmatrix}a_1^1\\a_1^2\end{pmatrix}=\begin{pmatrix}d-c\\f-e\end{pmatrix}. \tag{16}$$

Similar equations will come up at the other three corners, and the coefficients a_1^i, a_4^i of $x_i(t)$ $(i=1,2,3,4)$ can be determined from these equations, the other coefficients a_2^i and a_3^i can be freely chosen.

4.2. B-spline expression of the interpolation surface patch

In order to express the interpolation surface in B-spline form, firstly, $\boldsymbol{D}_i(t)$ should be expressed in B-spline form. Let $\Delta P_{j_1}^i=\frac{4(P_{j_1+1}^i-P_{j_1}^i)}{t_{j_1+5}^i-t_{j_1+1}^i}$, $\Delta^2P_{j_2}^i=\frac{3(\Delta P_{j_2+1}^i-\Delta P_{j_2}^i)}{t_{j_2+5}^i-t_{j_2+2}^i}$. Using the product formula of B-spline [15], we have

$$\boldsymbol{r}_i'(t)\times\boldsymbol{r}_i''(t)=\sum_{k=0}^{17}\overline{H}_k^iN_{k,5}(t)\quad\text{and}\quad x_i(t)\boldsymbol{r}_i'(t)=\sum_{k=0}^{17}F_k^iN_{k,5}(t), \tag{17}$$

where B-spline basis functions $N_{k,5}(t)$ defined on the knot vector $\overline{\boldsymbol{T}}_i$,

$$\overline{\boldsymbol{T}}_i=\{\underbrace{0,\ldots,0}_{6},\underbrace{t_5^i,\ldots,t_5^i}_{4},\underbrace{t_6^i,\ldots,t_6^i}_{4},\underbrace{t_7^i,\ldots,t_7^i}_{4},\underbrace{1,\ldots,1}_{6}\}=\{\bar{t}_0^i,\bar{t}_1^i,\ldots,\bar{t}_{23}^i\},$$

$$\overline{H}^i_k = \frac{1}{\binom{5}{3}} \sum_{P\in\prod} \sum_{j_1} \sum_{j_2} \alpha_{j_1,3,\boldsymbol{T}''_i,\boldsymbol{t}^P_i}(k)\alpha_{j_2,2,\boldsymbol{T}'_i,\boldsymbol{t}^Q_i}(k)\Delta P^i_{j_1} \times \Delta^2 P^i_{j_2},$$

$$F^i_k = \frac{1}{\binom{5}{3}} \sum_{P\in\prod} \sum_{j_1} \sum_{j} \Delta P^i_{j_1}\alpha_{j_1,3,\boldsymbol{T}''_i,\boldsymbol{t}^P_i}(k) a^i_j \alpha_{j,2,\boldsymbol{T}'_i,\boldsymbol{t}^Q_i}(k),$$

$$\boldsymbol{t}^P_i = \{\cdots, \bar{t}^i_k, \bar{t}^i_{k+p_1}, \bar{t}^i_{k+p_2}, \bar{t}^i_{k+p_3}, \bar{t}^i_{k+6}, \ldots\},$$

$$\boldsymbol{t}^Q_i = \{\cdots, \bar{t}^i_k, \bar{t}^i_{k+q_1}, \bar{t}^i_{k+q_2}, \bar{t}^i_{k+6}, \ldots\}.$$

$P = \{p_1, p_2, p_3\}$ is a selection of three integers from the set $I = \{1, 2, \ldots, 5\}$, and $Q = \{q_1, q_2\} = I - P$, $\prod$ is the set of all subsets of I consisting of three elements. $\alpha_{j_1,3,\boldsymbol{T}''_i,\boldsymbol{t}^P_i}$, $\alpha_{j_2,2,\boldsymbol{T}'_i,\boldsymbol{t}^Q_i}$ and $\alpha_{j,2,\boldsymbol{T}'_i,\boldsymbol{t}^Q_i}$ are the discrete B-splines.

Notice that the actual degree of $\boldsymbol{r}'_i(t) \times \boldsymbol{r}''_i(t)$ is of 4, that is,

$$\boldsymbol{r}'_i(t) \times \boldsymbol{r}''_i(t) = \sum_{m=0}^{13} H^i_m N_{m,4}(t).$$

$N_{m,4}(t)$ defined on the knot vector $\overline{\boldsymbol{T}}'_i = \{\underbrace{0,\ldots,0}_{5}, \underbrace{t^i_5,\ldots,t^i_5}_{3}, \underbrace{t^i_6,\ldots,t^i_6}_{3}, \underbrace{t^i_7,\ldots,t^i_7}_{3}, \underbrace{1,\ldots,1}_{5}\}$, and H^i_m can be obtained through the following method (for more details, see [16]).

$$P^{j-1}_k = \begin{cases} P^j_k, & 0 \le k \le l_j - 5, \\ \dfrac{1}{1-a^j_{k,4}} P^j_k - \dfrac{a^j_{k,4}}{1-a^j_{k,4}} P^{j-1}_{k-1}, & l_j - 4 \le k \le l_j - 1, \\ P^j_{k+1}, & l_j \le k \le 12 + j, \end{cases}$$

where $j = 4, 3, 2, 1$, $l_4 = 17$, $l_{j-1} = l_j - 4$, $P^4_k = \overline{H}^i_k$, $k = 0, \ldots, 17$, $H^i_m = P^0_m$, $m = 0, \ldots, 13$.

Then, using the product formula of B-spline again [15], we have

$$y_i(t)\boldsymbol{r}'_i(t) \times \boldsymbol{r}''_i(t) = \sum_{k=0}^{17} G^i_k N_{k,5}(t), \tag{18}$$

where $G^i_k = \sum_{P\in\prod}\sum_j\sum_m b^i_j \alpha_{j,1,\boldsymbol{T}_0,\boldsymbol{t}^P_i}(k) H^i_m \alpha_{m,4,\overline{\boldsymbol{T}}'_i,\boldsymbol{t}^Q_i}(k)/\binom{5}{1}$.

From (17) and (18), $\boldsymbol{D}_i(t)$ can be expressed as

$$\boldsymbol{D}_i(t) = \sum_{k=0}^{17} (F^i_k + G^i_k) N_{k,5}(t). \tag{19}$$

Because $\boldsymbol{D}_i(t)$ is of degree 5, we can define an interpolation B-spline patch with degree $(5, 5)$ as

$$\boldsymbol{R}(u, v) = \sum_{i=0}^{17}\sum_{j=0}^{17} D_{ij} N_{i,5}(u) N_{j,5}(v). \tag{20}$$

$N_{i,5}(u)$ defined on the knot vector $\overline{\boldsymbol{T}}_1$, $N_{j,5}(v)$ defined on the knot vector $\overline{\boldsymbol{T}}_2$.

Using the degree elevation formula of B-spline curves [15], we rewrite $\boldsymbol{r}_i(t)$ as

$$\boldsymbol{r}_i(t) = \sum_{k=0}^{17} \boldsymbol{d}^i_k N_{k,5}(t),$$

where

$$\boldsymbol{d}^i_k = \sum_j P^i_j \Lambda_{j,4,5,\boldsymbol{T}_i,\overline{\boldsymbol{T}}_i}(k),$$

$$\Lambda_{j,k_1,k_2,\boldsymbol{T}_i,\overline{\boldsymbol{T}}_i}(k) = \frac{k_1}{k_2}[\omega_{j,k_1,\boldsymbol{T}_i}(\bar{t}^i_{k+k_2})\Lambda_{j,k_1-1,k_2-1,\boldsymbol{T}_i,\overline{\boldsymbol{T}}_i}(k) + (1-\omega_{j+1,k_1,\boldsymbol{T}_i}(\bar{t}^i_{k+k_2}))\Lambda_{j+1,k_1-1,k_2-1,\boldsymbol{T}_i,\overline{\boldsymbol{T}}_i}(k)] + \frac{k_2-k_1}{k_2}\Lambda_{j,k_1,k_2-1,\boldsymbol{T}_i,\overline{\boldsymbol{T}}_i}(k)$$

for $k_2 > k_1$, and $\Lambda_{j,0,k_2,\boldsymbol{T}_i,\overline{\boldsymbol{T}}_i}(k) = \alpha_{j,0,\boldsymbol{T}_i,\overline{\boldsymbol{T}}_i}(k)$, $\Lambda_{j,k_1,k_1,\boldsymbol{T}_i,\overline{\boldsymbol{T}}_i}(k) = \alpha_{j,k_1,\boldsymbol{T}_i,\overline{\boldsymbol{T}}_i}(k)$,

$$\omega_{j,k_1,\boldsymbol{T}_i}(t) = \begin{cases} \dfrac{t - t^i_j}{t^i_{j+k_1} - t^i_j}, & \text{if } t^i_j < t^i_{j+k_1}, \\ 0, & \text{otherwise.} \end{cases}$$

It is obvious that

$$\begin{cases} D_{i0} = \boldsymbol{d}_i^1, & D_{i,17} = \boldsymbol{d}_i^3, \quad i = 0, 1, \ldots, 17, \\ D_{0j} = \boldsymbol{d}_j^2, & D_{17,j} = \boldsymbol{d}_j^4, \quad j = 0, 1, \ldots, 17. \end{cases} \tag{21}$$

By calculating directly the transverse tangent vector of $\boldsymbol{R}(u, v)$, and using (19) and (21), we have

$$\begin{cases} D_{i1} = \boldsymbol{d}_i^1 + \dfrac{v_5}{5}(F_i^1 + G_i^1), & \\ D_{1j} = \boldsymbol{d}_j^2 + \dfrac{u_5}{5}(F_j^2 + G_j^2), & i = 0, 1, \ldots, 17, \\ D_{i,16} = \boldsymbol{d}_i^3 - \dfrac{1 - v_7}{5}(F_i^3 + G_i^3), & j = 0, 1, \ldots, 17. \\ D_{16,j} = \boldsymbol{d}_j^4 - \dfrac{1 - u_7}{5}(F_j^4 + G_j^4). & \end{cases} \tag{22}$$

Notice that, the twist points of $\boldsymbol{R}(u, v)$ are calculated twice in (22), but they are compatible when relation (15) holds.

We can now state the following result.

Theorem 2. *For a four-quartic B-spline curvilinear quadrilateral constructed by the method in Section 3.2, if the first two lines of control points of the surface (20) satisfy (21) and (22), then the surface interpolates the quadrilateral as boundary geodesic quadrilateral.*

Theorem 2 indicates that the geodesic interpolation conditions only influence the first two lines of control points, the other inner control points being free. In order to smooth the surface, we choose the free control points by minimizing the following thin plate spline energy.

$$\min_{D_{ij}} E = \int_0^1 \int_0^1 (\|\boldsymbol{R}_{uu}(u, v)\|^2 + 2\|\boldsymbol{R}_{uv}(u, v)\|^2 + \|\boldsymbol{R}_{vv}(u, v)\|^2) du dv.$$

Let $\frac{\partial E}{\partial D_{ij}} = 0$, $i, j = 2, \ldots, 15$, we have

$$\sum_{0 \le k \le 17, k \ne i,} \sum_{0 \le l \le 17, l \ne j} D_{kl} M_{i,j,k,l} + D_{ij} M_{i,j,i,j} = 0, \tag{23}$$

where

$$M_{i,j,k,l} = \int_0^1 \int_0^1 \begin{pmatrix} N''_{i,5}(u) N_{j,5}(v) N''_{k,5}(u) N_{l,5}(v) \\ +2N'_{i,5}(u) N'_{j,5}(v) N'_{k,5}(u) N'_{l,5}(v) \\ +N_{i,5}(u) N''_{j,5}(v) N_{k,5}(u) N''_{l,5}(v) \end{pmatrix} du dv.$$

Then the free control points D_{ij} $(i, j = 2, \ldots, 15)$ can be obtained by solving the linear equation (23).

Based on the above analysis, the B-spline surface, which interpolates the constructed quadrilateral as boundary geodesic quadrilateral, can be constructed by the following steps.

(1) *According to the compatibility of the tangent and twist vector at the corners in* Section 4.1, $x_i(t)$ *and* $y_i(t)$ *are determined.*
(2) *From* (19), *we can calculate the control points of* $\boldsymbol{D}_i(t)$.
(3) *The control points of the interpolation patch, which are related with the geodesic interpolation condition, are calculated by* (21) and (22).
(4) *The remaining control points of the interpolation patch are obtained by solving the linear equation* (23).

Figs. 4–6 show three B-spline surfaces with degree (5, 5) interpolating the constructed quadrilaterals (Fig. 3(a–c)) as boundary geodesic quadrilateral, respectively.

5. Conclusion

In this paper, we propose an optimized geometric method to construct a four-quartic B-spline curvilinear quadrilateral satisfying the constraints of the crossing geodesics on a surface. For the constructed quadrilateral, a tensor-product B-spline surface of degree (5, 5) can be constructed to interpolate these curves as boundary geodesic quadrilateral. The scheme incurs the free control points, which can be used to smooth the interpolation surface. The interpolation surface patch adheres to the NURBS standard and employs geometric shape handles, such as control points, which is compatible with commercial CAD systems.

Acknowledgments

The authors are very grateful to the referees for their helpful suggestions and comments. This work is supported by the National Natural Science Foundation of China (Grant Nos. 61462036, 61272300) and the Natural Science Foundation of Jiangxi Province, China (No. 20151BAB201015).

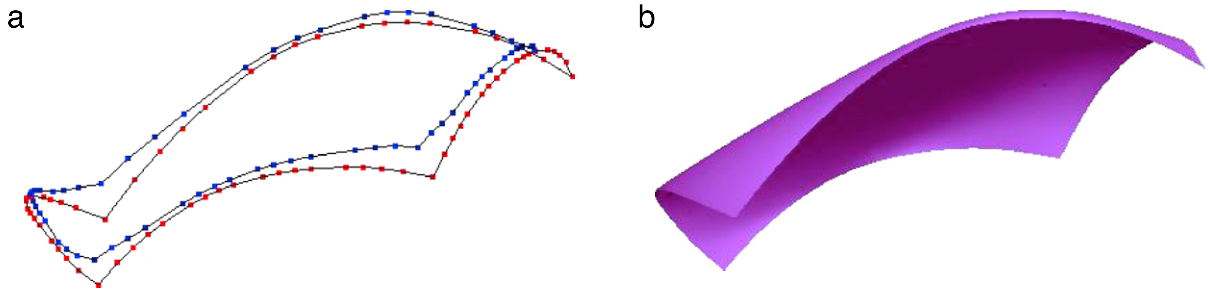

Fig. 4. Principal normal vector with no reversal. (a) The first two lines of control points. (b) Interpolation surface.

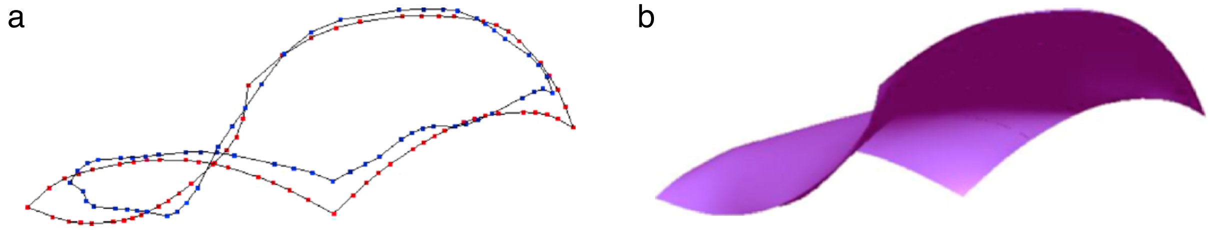

Fig. 5. Principal normal vector with two reversals. (a) The first two lines of control points. (b) Interpolation surface.

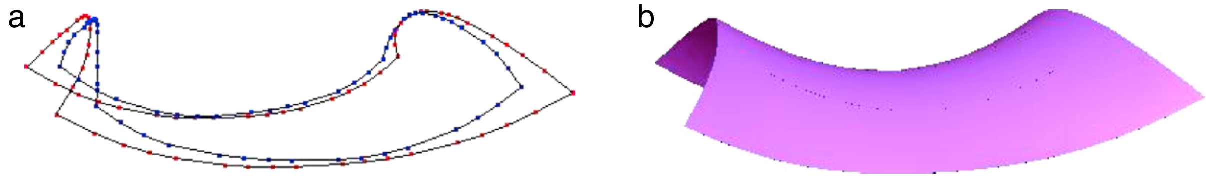

Fig. 6. Principal normal vector with four reversals. (a) The first two lines of control points. (b) Interpolation surface.

References

[1] C.L. Tucker III, Forming of advanced composites, in: T.G. Gutowski (Ed.), Advanced Composites Manufacturing, Wiley, New York, 1997, pp. 297–372.
[2] R.J. Haw, An application of geodesic curves to sail design, Comput. Graph. Forum 4 (2) (1985) 137–139.
[3] G.J. Wang, K. Tang, C.L. Tai, Parametric representation of a surface pencil with a common spatial geodesic, Comput.-Aided Des. 36 (5) (2004) 447–459.
[4] N. Sprynski, N. Szafran, B. Lacolle, L. Biard, Surface reconstruction via geodesic interpolation, Comput.-Aided Des. 40 (4) (2008) 480–492.
[5] M. Paluszny, Cubic polynomial patches through geodesics, Comput.-Aided Des. 40 (1) (2008) 56–61.
[6] J. Sánchez-Reyes, R. Dorado, Constrained design of polynomial surfaces from geodesic curves, Comput.-Aided Des. 40 (1) (2008) 49–55.
[7] C.Y. Li, R.H. Wang, C.G. Zhu, Designing and G^1 connection of developable surfaces through Bézier geodesics, Appl. Math. Comput. 218 (2011) 3199–3208.
[8] C.Y. Li, R.H. Wang, C.G. Zhu, Designing approximation minimal parametric surfaces with geodesics, Appl. Math. Model. 37 (2013) 6415–6424.
[9] H. Hagen, Geometric surface patches without twist constraints, Comput. Aided Geom. Design 3 (3) (1986) 179–184.
[10] R.T. Farouki, N. Szafran, L. Biard, Existence conditions for Coons patches interpolating geodesic boundary curves, Comput. Aided Geom. Design 26 (5) (2009) 599–614.
[11] R.T. Farouki, N. Szafran, L. Biard, Construction of Bézier surface patches with Bézier curves as geodesic boundaries, Comput.-Aided Des. 41 (11) (2009) 772–781.
[12] R.T. Farouki, N. Szafran, L. Biard, Construction and smoothing of triangular Coons patches with geodesic boundary curves, Comput. Aided Geom. Design 27 (4) (2010) 301–312.
[13] J.H. Yong, F.H. Cheng, Geometric Hermite curves with minimum strain energy, Comput. Aided Geom. Design 21 (3) (2004) 281–301.
[14] G. Farin, Curves and Surfaces for CAGD, fifth ed., Academic Press, Boston, 2002.
[15] K. Mørken, Some identities for products and degree raising of splines, Constr. Approx. 7 (1) (1991) 195–208.
[16] G.Z. Wang, C.Y. Deng, On the degree elevation of B-spline curves and corner cutting, Comput. Aided Geom. Design 24 (2) (2007) 90–98.